

Detection of nonlinear structural behavior using time-frequency and multivariate analysis

J. Prawin^a and A. Rama Mohan Rao^{*}

Academy of Scientific and Innovative Research, CSIR-Structural Engineering Research Centre,
CSIR Campus, Chennai, TN, India

(Received March 22, 2018, Revised August 23, 2018, Accepted September 29, 2018)

Abstract. Most of the practical engineering structures exhibit nonlinearity due to nonlinear dynamic characteristics of structural joints, nonlinear boundary conditions and nonlinear material properties. Hence, it is highly desirable to detect and characterize the nonlinearity present in the system in order to assess the true behaviour of the structural system. Further, these identified nonlinear features can be effectively used for damage diagnosis during structural health monitoring. In this paper, we focus on the detection of the nonlinearity present in the system by confining our discussion to only a few selective time-frequency analysis and multivariate analysis based techniques. Both damage induced nonlinearity and inherent structural nonlinearity in healthy systems are considered. The strengths and weakness of various techniques for nonlinear detection are investigated through numerically simulated two different classes of nonlinear problems. These numerical results are complemented with the experimental data to demonstrate its suitability to the practical problems.

Keywords: nonlinear systems; wavelets; Hilbert-Huang transform; principal component analysis; Holder exponent; null subspace analysis

1. Introduction

Identifying the damage-sensitive features that can accurately distinguish a damaged structure from an undamaged one is the focus of the most of the SHM technical literature (Sohn *et al.* 2002). Many existing SHM feature extraction methodologies for damage diagnosis are based on fitting linear models (e.g. modal models, physics-based models or data-based time-series model) to measured system response data before and after damage. Changes in the parameters or predictive errors of these models are then used as indicators of damage.

Change in the stiffness of the structure locally, that result in loss of performance is generally construed as damage. In many cases, a structure, which exhibits predominantly stationary and linear dynamic response properties in its undamaged state, tend to exhibit non-stationary and nonlinear properties after damage. Examples include post-buckled structures (Duffing non-linearity), rattling joints (impacting system with discontinuities), or breathing cracks (bilinear stiffness), delaminations, etc., and such damage has been referred to as damage with nonlinear features (Kerschen *et al.* 2006, Worden *et al.* 2001, 2008).

The damage detection process can be significantly enhanced if one takes advantage of these nonlinear effects when extracting damage-sensitive features from measured data.

Apart from this, several engineering structures are constructed with joints, geometric discontinuities and also built with shock absorbers, dampers etc. The enhancement of the stiffness and damping properties of a linear structure via structural modification through the addition of strongly nonlinear structural modules that behave, in essence, as Nonlinear Energy Sinks (Sapsis *et al.* 2012). Properly designed Nonlinear Energy Sinks can affect significantly the stiffness and damping properties of the structures to which they are attached. Apart from this, the structures can also have regions undergoing large displacements. Such structures exhibit localized nonlinearity while leaving some portions of the structure largely unaffected. However, these localized nonlinearities can have a significant global impact and they exhibit nonlinear behaviour even in the healthy state. The dynamic signatures obtained from these structures with localized nonlinearity will obviously have nonlinear features often mislead for a probable damage. Hence it is essential to take into account the contributions of these inherent localized nonlinearities to the dynamic signature and extract the additional features which can be attributed to damage in order to improve the robustness of the damage diagnostic algorithms for engineering structures. Therefore, a robust and reliable SHM system that can deal with both damage induced nonlinearity and inherent nonlinearities in healthy structures is highly desirable.

Several methods have been developed for detecting the presence of nonlinearity in a system (Wang *et al.* 2015, Casciati *et al.* 2016, Kerschen *et al.* 2006, Worden *et al.* 2000, 2008, Prawin and Rao 2017, 2018a, b, Sapsis *et al.* 2012, Pai *et al.* 2013, Hickey *et al.* 2009). These methods can be broadly classified as time domain (Worden and

*Corresponding author, Ph.D., Chief Scientist
E-mail: arm2956@yahoo.com

^a Ph.D. Scientist

Tomlinson 2000, Prawin and Rao 2017, Sapsis *et al.* 2012, Pai *et al.* 2013) modal analysis method (Hickey *et al.* 2009), frequency domain methods (Prawin and Rao 2017, Sapsis *et al.* 2012, Pai *et al.* 2013, Hickey *et al.* 2009), time-frequency analysis based techniques (Nagarajaih *et al.* 2015, Li *et al.* 2017, Bae *et al.* 2017, Robertson *et al.* 2003, 2013, Gokhale and Khanduja 2010, Goggins *et al.* 2007, Huang *et al.* 1998, Feldman 2011) and multivariate analysis techniques (Hot *et al.* 2012, Salehi *et al.* 2016, Hasselman *et al.* 1998, Cammarata *et al.* 2010, Zang *et al.* 2001, Yan and Golinval 2006, Rao *et al.* 2015). There is not a single technique available to handle all classes of nonlinear systems.

Modal parameters cannot be used directly for nonlinearity detection as they vary for different inputs and different input amplitudes. Even though the popular nonlinear modal analysis technique widely referred as Nonlinear Normal modes can be used for detection and even characterization. It requires a huge amount of data and involves complex mathematical operations.

Most of the well-known techniques use frequency domain data. The techniques such as Frequency Response Function (FRF) Distortions and Homogeneity test of FRF and Higher-order nonlinear frequency response function used for nonlinear detection are highly dependent on the excitation type. Hence they are not suitable for ambient variant data. The frequency domain data involves transformation and leakage errors. The frequency domain data is also highly sensitive to damping and noise.

The time domain techniques such as auto and cross-correlation cannot be primarily used to detect nonlinearity due to their sensitivity to measurement noise. Apart from this, harmonic distortion based nonlinear indicator uses harmonic excitation vibration data.

The main feature of the nonlinear vibration signal is that instantaneous parameters (i.e., both frequency and damping) are time varying function with respect to the different types of nonlinearity. Hence the feature extraction process requires analyzing the nonlinear and non-stationary signals. Majority of the time and frequency domain nonlinear detection techniques requires input force information and uses either sweep or harmonic excitation to detect the presence of nonlinearity. Even though there are few techniques, which use only ambient vibration data, they are highly susceptible to measurement noise. Further, for civil structures, it is often more convenient to measure the ambient vibration data than forced response data. Therefore, the time-frequency and multivariate analysis are promising tools to solve such non-stationary signals and to estimate the time-varying properties of the signal and detect the presence of nonlinearity in the system using ambient vibration data.

In view of this, in this paper, we present the investigations carried out on various time-frequency and multivariate analysis based nonlinear indicators for detection of nonlinearity in civil engineering structures using ambient vibration data. Both damage induced nonlinearity and inherent structural nonlinearity in healthy systems are considered. The selected time-frequency analysis based techniques include Holder Exponent,

Wavelet Packet Decomposition and Hilbert Huang Transform, while the multivariate analysis techniques include principal component analysis and null subspace analysis. Even though these methods have been investigated earlier by researchers for nonlinear detection, their capability for both classes of nonlinear problems with ambient excitation is not fully exploited. In addition, an attempt is also made in this paper to reflect the strengths and weakness of these techniques with ambient excitation and sensitivity to noise through experimental and numerically simulated examples. In the present work, these existing time and time-frequency domain techniques are evaluated with respect to the identification of presence of nonlinearity in the structure, identification of time instant of incipience of nonlinearity, sensitivity to noise, applicability to two different classes of nonlinearity.

2. Nonlinear detection techniques

In this section, we present the details related to the various time-frequency and multivariate analysis techniques considered in this paper for nonlinear detection with ambient vibration data.

2.1 Holder exponent

Holder exponent is usually used to assess the signal regularity in time. The regularity identifies the degree to which the signal is differentiable. Conventionally, Holder exponent is found from the Fourier transform of the signal, which will only provide global minimum regularity. However, with wavelet analysis, the signal regularity is assessed at multiple time measurements. The wavelet variability of time and frequency in the wavelet analysis provides a finer time resolution at the higher frequencies, which can be useful to detect when sudden changes in the signal occur. Therefore, Holder exponent is determined using wavelet analysis in the present work.

$$|Wf(u,s)| = \left| \int_{-\infty}^{\infty} f(t) \frac{1}{\sqrt{s}} \psi^* \left(\frac{t-u}{s} \right) dt \right| \quad (1)$$

The Holder exponent is determined by applying the wavelet transform of the structure response signal (acceleration time history data) to calculate the absolute values of the resulting wavelet coefficients. Then these coefficients are organised in a two-dimensional time-scale matrix. While the first dimension of the time-scale matrix (u) represents a different time point in the signal, the other dimension denotes a different frequency scale (s). Extract one column at a time from the time-scale matrix. Each column is the frequency spectrum of the signal at a particular time instant. Generate a log-log plot of this extracted vector at each point of time with the corresponding scale. The slope of this line provides the Holder exponent at a particular time point (Robertson *et al.* 2003).

The measurement of signal regularity using holder exponent can be used to detect singularities (or

discontinuities) induced by the nonlinearity present in the structure. The easiest way to identify discontinuity induced by nonlinearity using Holder Exponent is the change in the regularity (Holder exponent) versus time. A discontinuous point has a Holder exponent value of zero, however resolution limitations of the wavelet transform will result in slightly different values from zero. So, identifying time points where the Holder exponent decreases from positive values towards zero, or below, will identify when the discontinuities in the signal occur. From this, the nonlinearities induced in the form of discontinuities into the measured dynamic response data can be identified.

Once holder exponent values are extracted, the threshold value or control limit is employed, which exceedance will indicate the presence of nonlinearity in the system. The control limit is determined using known data with no discontinuities (i.e., linear response). In order to apply the control limit, all the local maxima and minima of the Holder exponent function in time for the normal signal (linear data) are first recorded and then the drops in the Holder exponent values are calculated as the difference between a given minimum and the maximum immediately preceding it. The control limit is typically set at 1.5 times of the greatest decrease of the holder exponent value under linear conditions. The threshold of 1.5 is derived using extreme value statistics chosen (Robertson *et al.* 2003, 2013). It is essential to have the acquired reference linear response of the structure to develop statistical classifiers for Holder exponent to detect the presence of such discontinuities. If the Holder exponent of the test data is greater than the control limit, the presence of nonlinearity is identified. To remove excess of noise, low-pass moving average (MA) filter is applied.

2.2 Wavelet Packet Decomposition

The Wavelet Packet Decomposition (WPD) is a generalization of wavelet decomposition that provides a wider range of possibilities for signal analysis. Using wavelet packet decomposition, level by level transformation of a signal from time domain to frequency domain can be achieved. In order to reduce the time resolution and increase the frequency resolution, Wavelet Packet Decomposition (WPD) uses a recursion of filter-decimation operations (Gokhale and Khanduja 2010). Since the WPD divides not only the low but also the high-frequency sub-band, the frequency bands are of equal width, unlike wavelet decomposition.

In wavelet analysis, a signal is split into approximation and detail coefficients. The approximation coefficients are split into a second-level approximation and detail coefficients. In wavelet packet analysis, the detail and approximation coefficients can be split. This results in more than $2^{2^{n-1}}$ different ways to encode the signal.

When the wavelet transform is generalized to the wavelet packet transform, not only can the low pass filter output be iterated through further filtering, but the high pass filter can be iterated as well. This ability to iterate the high pass filter outputs means that the wavelet packet transform allows for more than one basis function (or wavelet packet)

at a given scale while the Wavelet Transform has one basis function at each scale other than the deepest level, where it has two. The set of wavelet packets collectively makes up the complete family of possible bases, and many potential bases can be constructed from them. If only the low pass filter is iterated, the result is the wavelet basis. If all low pass and high pass filters are iterated, the complete tree basis is constructed. The uppermost level of the WPD tree is the time representation of the signal. As each level of the tree is traversed there is an increase in the tradeoff between time and frequency resolution. The bottom level of a fully decomposed tree is the frequency representation of the signal.

Since Wavelet Packet Transform is a level by level decomposition technique, a total number of 2^j components can be derived if the signal is decomposed to j^{th} level. Each component has a central frequency determined for i^{th} wavelet packet component from

$$f_i = \frac{(2i - 1)f_N}{2^{j+1}} \quad (2)$$

The central frequency f_i of the i^{th} component at level j is represented in terms of Nyquist frequency f_N , which is determined as the half of the sampling frequency. Once the dynamic signals (i.e., acceleration time history response) measured from structures are decomposed into the wavelet packet components. Then the wavelet packet component energy will be estimated. The component energy is calculated as

$$e_{j,n} = \sum_k c_{j,n}^2 \quad (3)$$

where 'e' represents the component energy at the j^{th} level at the n^{th} node. Notation 'c' represents the wavelet packet coefficient and 'k' is the translation parameter. The wavelet packet component energy basically measures the signal energy content for a specific frequency band. For the given wavelet basis and decomposition level, the wavelet transform of a signal is unique and invariant. Therefore, the wavelet packet transforms energy values extracted from the decomposed signals will also be unique for the linear system and can be used as a feature to represent the system characteristics. The shifts of wavelet packet component energy amongst frequency band can be employed as a feature to detect the presence of nonlinearity in the structure (Goggins *et al.* 2007, Shahverdi *et al.* 2013). This is because the nonlinearity present in the structure will suppress or enhance certain frequency components of the structure response signal.

2.3 Instantaneous frequency

Instantaneous frequency is defined as the rate of change of the phase angle at time t of the analytic version of the signal. Given a real signal $x(t)$, the analytic signal $z(t)$ is a complex signal having the actual signal as the real part and the Hilbert transform of the signal as the imaginary component. In order to perform the Hilbert transform, first, the time history signal needs to be decomposed into monocomponent signals called intrinsic mode function (IMF) using empirical mode decomposition (EMD). Details related to Empirical Mode Decomposition can be found in Huang *et al.*, 1998, Feldman (2011) . Once, the IMF

components from the time history $x(t)$ are obtained using EMD, Hilbert transform on each IMF $C_j(t)$ can be applied to determine the following set of equations below

$$\bar{C}_j(t) = \frac{1}{\pi} P \int_{-\infty}^{\infty} \frac{C_j(\tau)}{t - \tau} d\tau \quad (4)$$

$$z_j(t) = C_j(t) + i\bar{C}_j(t) = A(t)e^{i\theta(t)} \quad (5)$$

$$A(t) = \left[[C_j(t)]^2 + [\bar{C}_j(t)]^2 \right]^{1/2} \quad \text{and} \quad (6)$$

$$\theta(t) = \tan^{-1} \frac{\bar{C}_j(t)}{C_j(t)}$$

$$\omega(t) = \frac{d\theta(t)}{dt} \quad (7)$$

Where $A(t)$ is instantaneous amplitude, and $\theta(t)$ is the phase angle and $\omega(t)$ is the instantaneous frequency $\omega(t)$. With these set of equations, the Instantaneous frequency can be estimated. Structural properties of the linear system such as Instantaneous frequency do not vary with time. Hence the shift in the instantaneous frequency or time-varying nature of instantaneous frequency can be attributed to the presence of nonlinearity in the structure.

2.4 Principal component analysis

Principal Component Analysis (Hot *et al.* 2012, Khoshnoudian and Talaei 2017, Khoshnoudian and Bokaeian 2017, Kerschen *et al.* 2004) includes Singular Value Decomposition (SVD) on the time domain response data, A (an $m \times n$ matrix of data, n data points of m different measurements)

$$A = U\Sigma V^T \quad (8)$$

where U indicates the principal components (PCs) of size $m \times m$ and V indicates the principal coordinate history of size $n \times n$ respectively which contains the normalized frequency response of the principal directions. The diagonal matrix Σ is termed the singular matrix which represents the level of ‘energy’ present in each mode. The principal directions extracted from test data, always lie in the subspace (or hyperplane) generated by the participating modes for the healthy linear system. Mathematically speaking, this means that the so-called principal hyperplane is invariant, even if the directions of the principal vectors are dependent on the structural excitation. Nevertheless, the principal hyperplane is dependent on the structural characteristics. This can be effectively employed to detect the presence of nonlinearity, as the principal hyperplane will be altered with increased levels of excitation indicating the nonlinearity in the structure’s response.

The presence of nonlinearity can be detected using the subspace angle between baseline data, i.e., when the structure is linear and the current response when the structure exhibits nonlinearity (Golub and Loan 2012). Theoretically, if the response is linear, the angle between the subspaces spanned by reference data and the current data should be zero. In reality, it

will not be zero due to environmental variances and also the noises present in the measurement process. In view of this, a number of reference data set with the linear response at varied excitation levels are collected by taking measurements at different time instants and partitioned into several sets. This gives us a collection of different subspace angle values. It can easily verify that the subspace angles obtained for the linear system with environmental variability follow a normal distribution. Hence, we can establish the control limits using the data of subspace angles obtained from the linear structure. The presence of the nonlinearity in the structure can be detected when the subspace angle of the monitored current data exceeds the control limits.

Alternatively, the presence of nonlinearity can be detected through residual projection error after projecting one subspace on to the other. The residual projection error can then be calculated as

$$x_{NL}^*(t) = P P^T x_{NL}(t) \quad (9)$$

where P is the principal component matrix of the baseline data of size $m \times p$ (m -no. of sensors and ‘ p ’- no. of PCs extracted from U with 99.5% of total energy). Thus, for each time step, the projection error vector (Hot *et al.* 2012) is given as

$$r(t) = \left\| x_{NL}^*(t) - x_{NL}(t) \right\| \quad (10)$$

From the projection error vector $r(t)$ obtained at time t , the novelty index NI can be defined using Mahalanobis norm as

$$NI_t = \sqrt{r(t)^T M^{-1} r(t)} \quad (11)$$

Where $M = (1/n) X_{NL} X_{NL}^T$ is the covariance matrix. The nonlinearity can be detected through novelty index when the prediction error at any time increment exceeds the upper control limit corresponding to the Mahalanobis norm.

2.5 Null subspace analysis

In Null subspace analysis, the acceleration time history response measured in the form of a matrix of size $m \times n$ similar to PCA is partitioned into several data subsets, in the case of continuous online monitoring of the structure. A block Hankel matrix $H_{p,q}$ from the output covariance matrix can be formed for each data subset (Yan and Golinval 2006, Rao *et al.* 2015) and can be written as

$$H_{p,q} = \begin{bmatrix} \Lambda_0 & \Lambda_1 & \dots & \dots & \Lambda_{q-1} \\ \Lambda_1 & \Lambda_2 & \dots & \dots & \Lambda_q \\ \dots & \dots & \dots & \dots & \dots \\ \Lambda_{p-1} & \Lambda_p & \dots & \dots & \Lambda_{p+q-2} \end{bmatrix}; \quad (12)$$

$$q \geq p \text{ where } \Lambda_i \approx \frac{1}{(N-i)} \sum_{k=1}^{N-i} y_{k+i} y_k^T; \quad 0 \leq i \leq N-1$$

The indices p and q in the Hankel matrix define the number of considered time shifts and should be chosen based on the assumed system order n , i.e. $q = n - p + 1$ and Λ_i represents the output covariance matrix and $\{y\}$ is the acceleration time

history response of a particular sensor. y_k refers to the acceleration at k^{th} time step. Performing the singular-value decomposition (SVD) on the weighted Hankel matrix, we get

$$\begin{aligned} \bar{\mathbf{H}} &= \mathbf{W}_1 \mathbf{H}_{p,q} \mathbf{W}_2 \approx [\mathbf{U}_1 \quad \mathbf{U}_2] \begin{bmatrix} \mathbf{S}_1 & 0 \\ 0 & 0 \end{bmatrix} [\mathbf{V}_1 \quad \mathbf{V}_2]^T \\ &= \mathbf{U}_1 \mathbf{S}_1 \mathbf{V}_1^T \end{aligned} \quad (13)$$

where \mathbf{W}_1 and \mathbf{W}_2 are weighting matrices chosen as identity matrices for simplicity (Yan and Golinval 2006). Due to the orthonormal property of matrices, the following relationship can be written mathematically as

$$\mathbf{U}_2^T \mathbf{U}_1 = 0 \quad (14)$$

However, in reality, Eq. (14) will not be zero due to environmental variances, variation of the ambient excitation and measurement noise. Therefore, the residue matrix \mathbf{R}_s should be formulated and determined as the matrix obtained by multiplying the null space matrix ($\mathbf{U}_{L0,r}^T$) of the baseline data and the active subspace matrix ($\mathbf{U}_{L1,c}$) of the current data set

$$\mathbf{R}_s = \mathbf{U}_{2,r}^T \mathbf{U}_{1,c} \quad (15)$$

The residue matrix \mathbf{R}_s contains the information about how the new data obtained has been altered. The null subspace angle (NSA) or the complementary angle between subspaces \mathbf{U}_{20} and $\mathbf{U}_{1,c}$ can be employed as a measure to detect the presence of nonlinearity. It can be derived as follows.

$$\text{NSA} = \sin^{-1}[\text{norm}(\mathbf{R}_s)] \quad (16)$$

where $\text{norm}(\cdot)$ is an operator giving the maximal singular value of a matrix. A large value of null subspace angle indicates a change in the state of the system from linear to nonlinear. As earlier pointed out, the null subspace angle (NSA) cannot be equal to zero due to environmental noise. Similar to the PCA method, the NSA limit of linearity is also obtained using the procedure in section 2.4.

The degree of nonlinearity index (DoN) is derived from the residue matrix to quantify the severity of nonlinearity present in the system and it can be defined as follows

$$\text{DoN} = \frac{\|\{\beta\}_c\|}{\|\{\beta\}_r\|} \quad (17)$$

where $\|\cdot\|$ indicates the Euclidean norm and the vector $\{\beta\}$ having size $\{m_1 \times 1\}$ can be defined through absolute row sum of residue matrix \mathbf{R}_s of size $m_1 \times n_1$ as

$$\{\beta\} = \sum_{j=1}^{n_1} |\mathbf{R}_s^{(i,j)}| \quad \text{where } i = 1, 2, \dots, m_1 \quad (18)$$

The DoN value will be one when the system is linear and will be higher than one when the nonlinearity is present in the system and it can be taken as the intensity measure of nonlinearity in the system.

3. Numerical examples

In this paper, several time-frequency and multivariate analysis based techniques for detection of the presence of nonlinearity in the structures are presented. We have demonstrated the strengths and weaknesses of each of the techniques presented through carefully chosen two numerical examples exhibiting different classes of nonlinearity and the experimental simulations of a benchmark problem provided by the LANL (Los Alamos Laboratory) Structural Health Monitoring benchmark site. Among the two numerically simulated examples, the first one is a cantilever beam with a local nonlinear stiffness attachment which comes under the class of structural systems exhibiting inherent nonlinearity even in its initial healthy state. The second one is the cantilever beam with a breathing crack exhibiting nonlinearity only after damage (i.e., damage induced nonlinearity).

However, engineering structural systems usually exhibit nonlinear behaviour during service life due to operational and environmental loads. In order to simulate the real structure behaviour, i.e., the structure is initially linear and later become nonlinear, we propose to introduce nonlinearity after certain time steps for both class of nonlinear problems considered in this paper. This sort of simulation helps in verifying the effectiveness of the algorithm in identifying the exact time of incipience of nonlinearity.

3.1 Numerical example-1: Cantilever beam

The cantilever beam model as shown in Fig. 1 is considered (Hot *et al.* 2012). The span of the beam is 1.0m and the cross-sectional dimension is 0.014 X 0.014 m. The beam is modelled using 10 beam elements. A non-linear cubic spring K_{NL} is added between the beam free end and the ground. The material properties of the beam are Young's Modulus, $E = 2.1E11$ MPa; mass density, $\rho = 7800$ Kg/m³; Nonlinear spring stiffness, $K_{NL} = 1.0E07$ N/m³. The linear damping matrix is constructed using Rayleigh damping.

The non-linear force, F_{KNL} due to the nonlinear stiffness can be expressed as functions of the translational displacement of node 11 over y-direction

$$F_{KNL} = K_{NL} y_{11}^3 \quad (19)$$

The nonlinearity is introduced after 4500-time steps of beam's loading. The first five Eigen-frequencies of the underlying linear response of the beam are 11.73 Hz, 73.54 Hz, 205.96 Hz, 403.87 Hz and 668.67 Hz. The beam is excited with 0.35, 2, 6 and 100 NRMS on free end for about 1.2 Sec in the frequency band [1–800 Hz]. The time domain response is calculated using Newmark's (constant average acceleration) time integration scheme combined with the Newton-Raphson algorithm. The acceleration history of all active nodes, i.e., nodes 2 to 11 in Fig. 1 is considered. The response corresponding to the very low amplitude of excitation i.e., 0.35NRMS, exhibiting linear behaviour is taken as the reference data. The chosen sampling frequency is 5000 Hz. In order to investigate the effect of the noise level on the performance of the proposed algorithm, environmental noise (i.e., white noise) is added to the

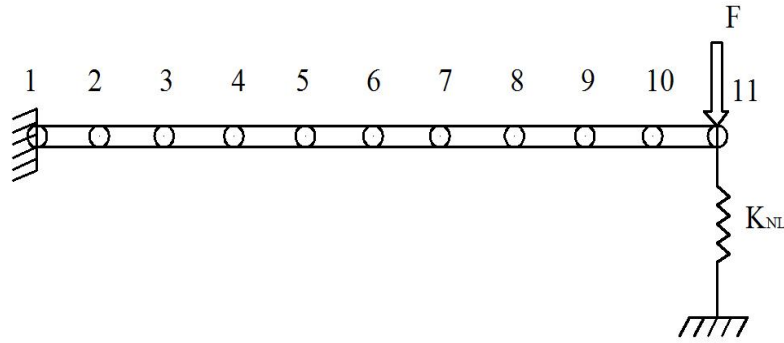


Fig. 1 Cantilever beam

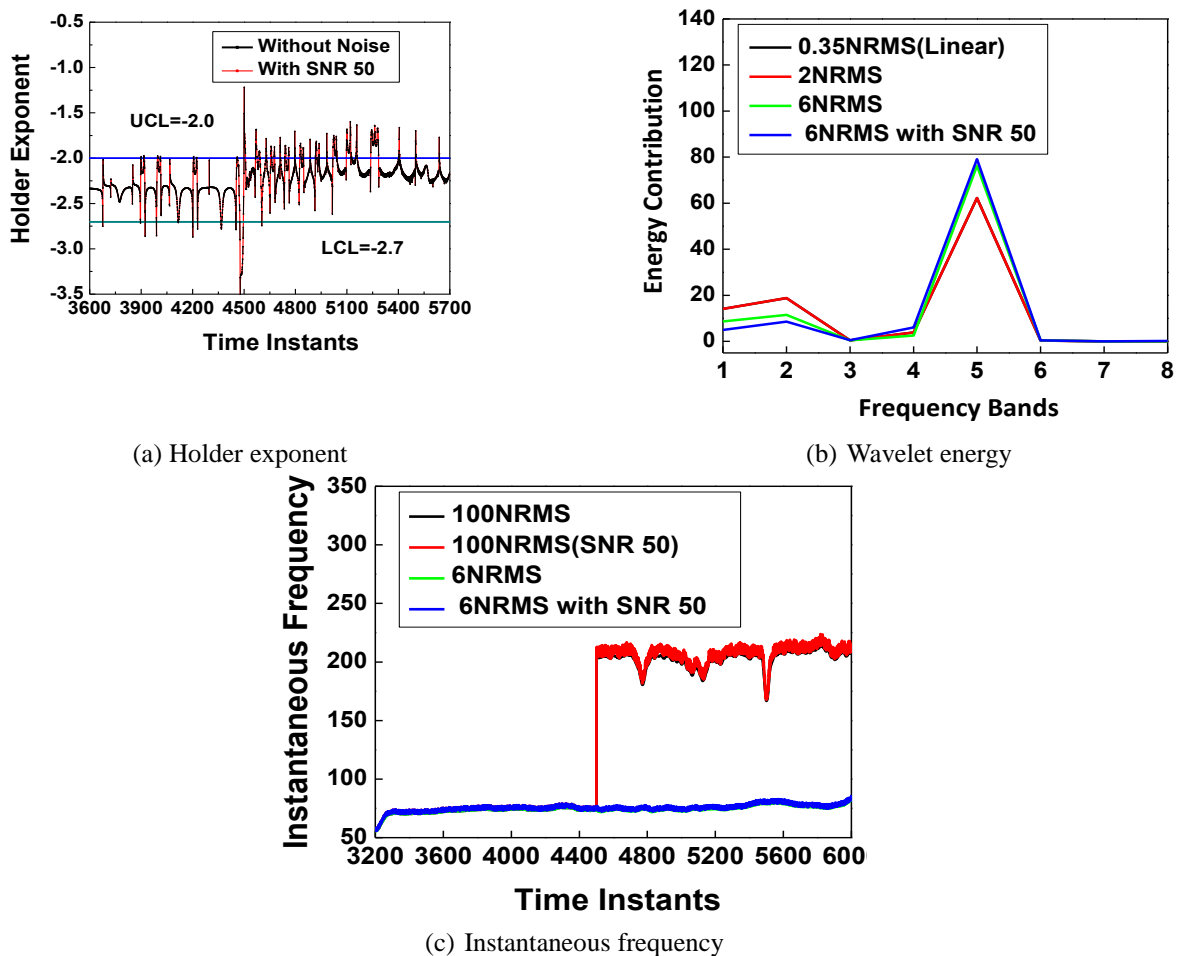


Fig. 2 Time-frequency analysis

acceleration time history before it is processed in the form of signal to noise ratio (SNR). We have considered SNR 50 for both the numerical examples considered in this paper.

The results from applying the time-frequency analysis based nonlinearity detection techniques in section 2 for the cantilever beam are shown in Fig. 2. The Holder exponent, WPT energy plot and instantaneous frequency plots are shown in Figs. 2(a)-2(c) respectively. The response measured at the free end is used for estimating the nonlinearity index proposed in various methods considered in this paper.

The discontinuity at the onset of nonlinearity at the 4500th time increment can be observed from the holder exponent plot shown in Fig. 2(a). The presence of nonlinearity is confirmed by the Holder exponent values crossing the limit of linearity after 4500th-time step. The results presented with applied noise in Fig. 2(a) show that this method is insensitive to noise.

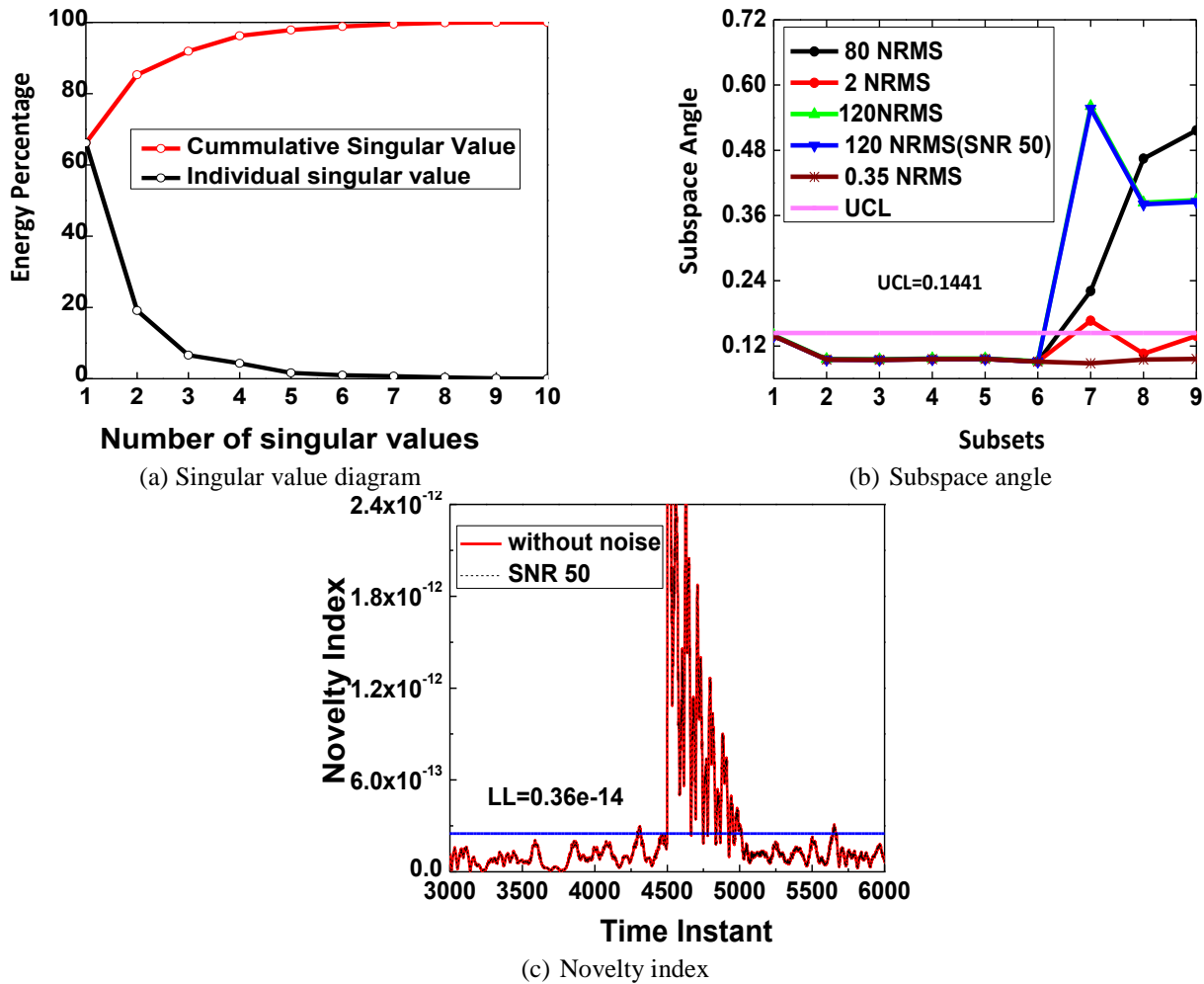


Fig. 3 Principal component analysis

The WPT energy plot shown in Fig. 2(b) for varied excitations levels clearly indicate that there is no variation in the energy (energy/frequency shifts) at a low level of excitations (NRMS) i.e., the system is in a linear state. However, we can observe marginal variation in the energy at high amplitude of excitation i.e., when the degree of nonlinearity present in the system is relatively high. From the range of excitations in Fig. 2(b), it is difficult to establish conclusively the presence of nonlinearity as the observed energy shifts can be also attributed to the temporal variation of the excitation frequency content. However, comparison of the WPT correlation coefficients of both excitation and response given in Tables 1 and 2 indicates the presence of nonlinearity. For the linear cantilever beam in Table 1, the correlation coefficient is close to 1 for all levels of excitation (also with imposed noise). However, the averaged WPT coefficients shown in Table 2, for the cantilever beam with introduced nonlinearity decrease with an increase in the level of excitation. This confirms the presence of nonlinearity in the system. In summary, wavelet packet energy together with WPT correlations can be used as an indicator for detecting the presence of nonlinearity. This method cannot give the exact time instant of nonlinearity.

From the instantaneous frequency results in Fig. 2(c), a shift in the frequency at the onset of nonlinearity (i.e., from the linear resonant frequency at 73 Hz to 75 Hz at 6NRMS excitation and to 180 Hz at 100NRMS excitation) is clearly visible. However, it is difficult to confirm the presence of nonlinearity at lower levels of excitation (i.e., low degree of nonlinearity) below 6 NRMS with and without noise. These smaller shifts can be even due to measurement noise. In order to confirm the presence of nonlinearity using Instantaneous frequency, it is essential that the degree of nonlinearity in the system should be high enough. This method identifies the exact time instant of nonlinearity.

The effectiveness of PCA based nonlinear detection methods based on subspace angles and prediction error based method are investigated and the results are shown in Fig. 3. The singular value diagram shown in Fig. 3(a) indicates that the first seven principal components contribute to 99.5% of energy cantilever beam. Hence, 7 PCs are used for evaluation.

The subspace angle plot for various levels of excitation of the cantilever beam is shown in Fig. 3(b). It can be observed that for the excitation level of 0.35NRMS, the beam behaviour is linear and hence the subspace angle is well below the upper control limit (UCL) and with an increase in the excitation levels to 2NRMS, 80NRMS and 120 NRMS, the subspace angles are

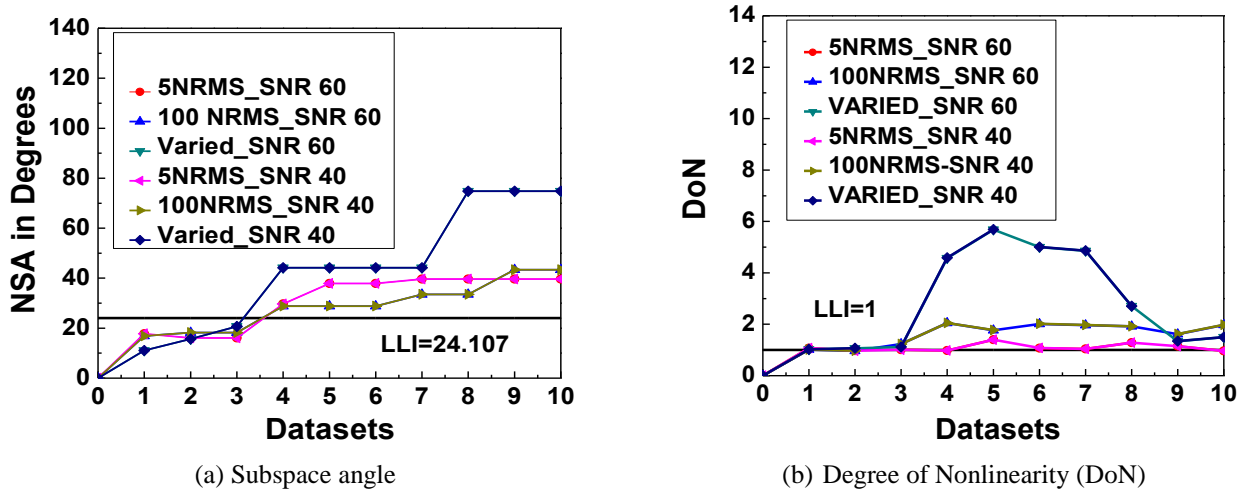


Fig. 4 Null subspace analysis

Table 1 WPT correlation of linear cantilever beam

| Level of Excitation | Frequency bands corresponding to the 3 rd level of WPT decomposition | | | | | | | | |
|---------------------|---|--------|--------|--------|--------|--------|--------|--------|----------|
| | 1 | 2 | 3 | 4 | 5 | 6 | 7 | 8 | Average |
| Low(2NRMS) | 1 | 1 | 1 | 1 | 1 | 1 | 1 | 1 | 1 |
| Medium(6NRMS) | 0.9287 | 0.9887 | 0.9764 | 0.9705 | 0.9387 | 0.9785 | 0.9418 | 0.9984 | 0.965213 |
| High(100NRMS) | 0.8171 | 0.8887 | 0.8677 | 0.7088 | 0.9007 | 0.9133 | 0.9865 | 0.9184 | 0.8751 |
| High (SNR50) | 0.8167 | 0.8886 | 0.8680 | 0.7088 | 0.9007 | 0.9132 | 0.9864 | 0.9184 | 0.8751 |

Table 2 WPT correlation of cantilever beam with stiffness nonlinearity

| Level of excitation | Frequency bands corresponding to the 3 rd level of WPT decomposition | | | | | | | | |
|---------------------|---|--------|--------|--------|--------|--------|--------|---------|----------|
| | 1 | 2 | 3 | 4 | 5 | 6 | 7 | 8 | Average |
| Low(2NRMS) | 0.6184 | 0.7944 | 0.3564 | 0.8545 | 0.0114 | 0.1069 | 0.1198 | 0.11054 | 0.371543 |
| Medium(6NRMS) | 0.6136 | 0.7943 | 0.3564 | 0.8545 | 0.0114 | 0.1070 | 0.1198 | 0.1105 | 0.370944 |
| High(100NRMS) | 0.5957 | 0.7938 | 0.3557 | 0.8543 | 0.0114 | 0.1070 | 0.1200 | 0.1105 | 0.368553 |
| High (SNR 50) | 0.5957 | 0.7938 | 0.3557 | 0.8543 | 0.0114 | 0.1070 | 0.1200 | 0.1105 | 0.36855 |

well above the control limit, clearly indicating the presence of nonlinearity. The exact time instant, where the system changes from linear to the nonlinear state can be identified from the control limits drawn when the subspace angle of any dataset with the earlier datasets exceeds the UCL. Alternatively, we can also establish the presence of nonlinearity using the projection error plots shown in Fig. 3(c). It can be observed that the novelty index plotted in Fig. 3(c), clearly overshoots the established limit of linearity at 4500th time step, clearly indicating the presence of nonlinearity.

Similarly, the results of the cantilever beam with null subspace analysis are shown in Fig. 4. It can be clearly observed from Fig. 4(a) that the subspace angle is well below the limit of linearity for the first three datasets due to linear behaviour and after the fourth dataset, the values crosses the limit of linearity. The angle is found to be increasing with increase in the excitation levels due to hardening behaviour. The exact time

instant, where the system changes from linear to the nonlinear state can be identified from the control limits established. Apart from this, we can quantify the degree of nonlinearity (DoN) present in the system using Null space analysis as shown in Fig. 4(b). It can be observed from Fig. 4(b) that the DoN index established (Eq. (17)) can precisely estimate the degree of nonlinearity present in the system, which can be used to judge the state of the system under varying levels of excitation.

In summary, all the time-frequency and multivariate analysis based techniques have the ability to identify inherent nonlinearity present in the structural system even in their healthy state. All the techniques except Wavelet Packet Component Energy exactly identify the time incipience of nonlinearity, hence amenable to online monitoring. It should be mentioned here that in order to confirm the presence of nonlinearity using instantaneous frequency, the degree of nonlinearity should be significant enough.

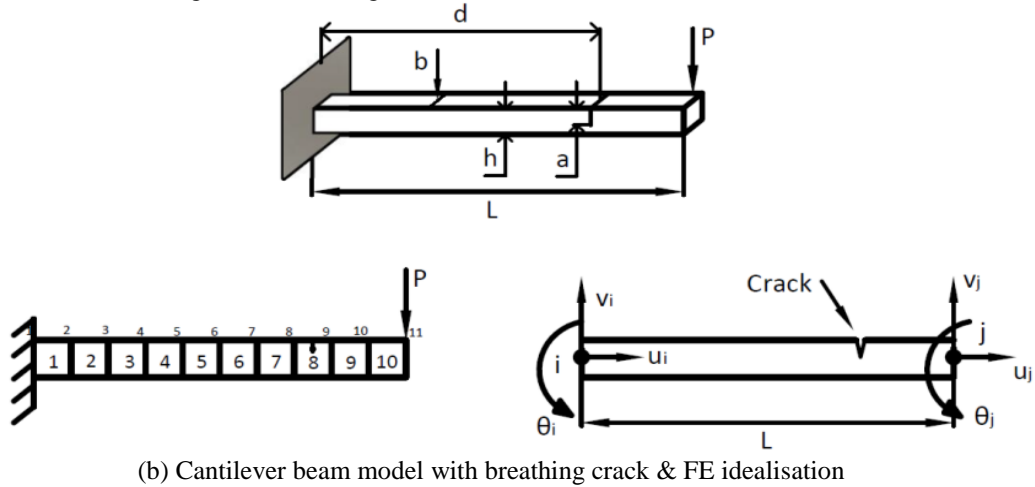
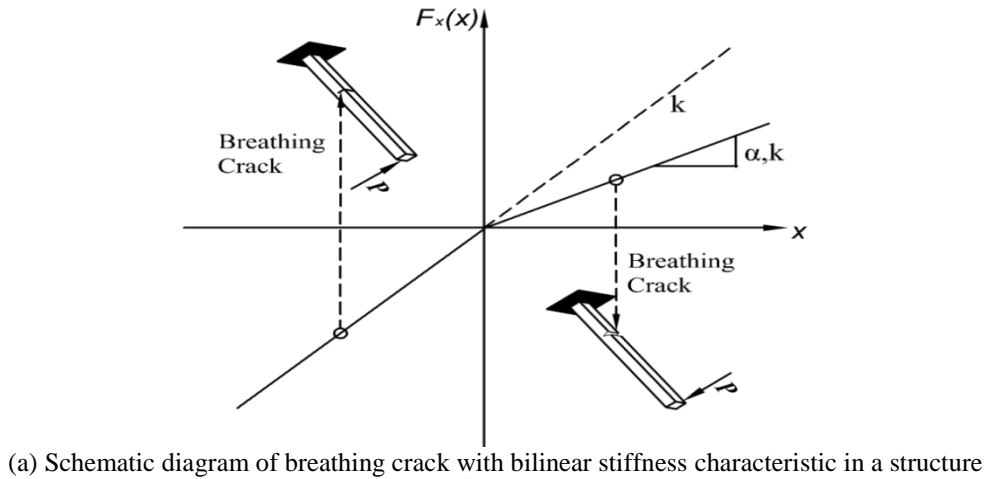


Fig. 5 Cantilever beam with a breathing crack

Both multivariate analysis technique and holder exponent requires reference linear response data to establish control limits, which exceedance confirms the presence of nonlinearity in the structure. Even though Wavelet Packet Component Energy does not require reference linear data, it requires a varied range of excitation responses and input force data to give a clear-cut conclusion about the presence of nonlinearity in the structure.

3.2 Numerical example 2: Breathing crack problem

The cantilever beam model with breathing crack shown in Fig. 5 is chosen as the second numerical example. The beam is initially in linear state and once the damage in the form of breathing crack sets in, the beam exhibits nonlinear behaviour. This comes under the class of damage induced nonlinearity problem. The span of the beam is 1.0 m and the cross-sectional dimension is 0.014 x 0.014 m. The material properties are: $E=2.1e11$ Pascal, $\rho= 7800$ kg/m³. The beam is discretized with 10 elements and simulated with a single-edged breathing crack at element no.5. Heavy side step function is widely used by the researchers to model bilinear stiffness behaviour (due to change in the state of the cracked domain from open to close and vice versa) of the breathing crack (Prawin *et al.* 2015, Giannini *et al.* 2013, Lim *et al.* 2017). In the present work, the same has been adopted. The cracked domain of the structure is initially assumed

to be in the closed state under compression and opening mechanism is triggered by the rotations at the nodes of the damaged element (i.e., θ_i, θ_j with breathing crack located between node i and j) when the cracked domain is under tension.

The actual stiffness K in the closed state is scaled by the factor α ($0 < \alpha < 1$) in open state of crack. The stiffness of the cracked domain is given by

$$K_d = K - H(\theta_i - \theta_j)K_c : \begin{cases} H(\theta_i - \theta_j) = 1, \theta_i > \theta_j \\ H(\theta_i - \theta_j) = 0, \theta_i < \theta_j \end{cases} \quad (20)$$

$$K_c = \frac{\mu E}{L} \begin{bmatrix} 0 & 0 & 0 & 0 & 0 & 0 \\ \frac{12I_u}{L^2} & \frac{6I_u}{L} & 0 & -\frac{12I_u}{L^2} & \frac{6I_u}{L} & 0 \\ 0 & 4I_u & 0 & -\frac{6I_u}{L} & 2I_u & 0 \\ 0 & 0 & 0 & 0 & 0 & 0 \\ sym & & & \frac{12I_u}{L^2} & -\frac{6I_u}{L} & 0 \\ 0 & 0 & 0 & 0 & 0 & 4I_u \end{bmatrix} \quad (21a)$$

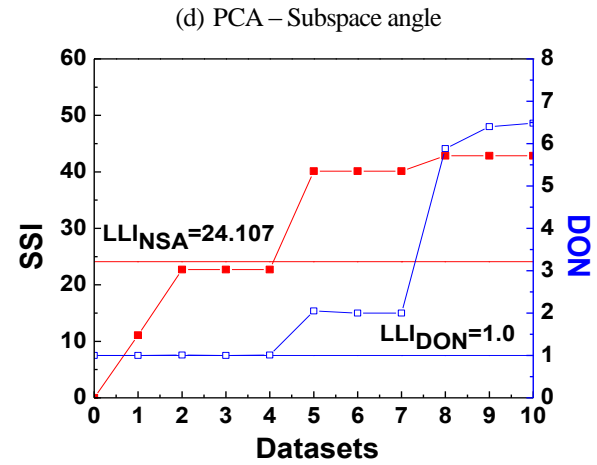
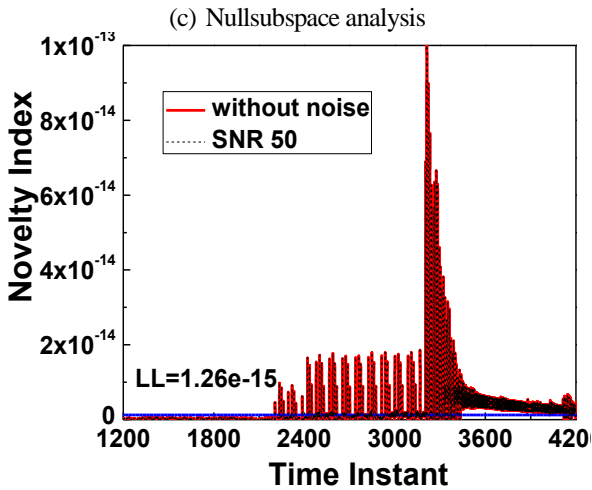
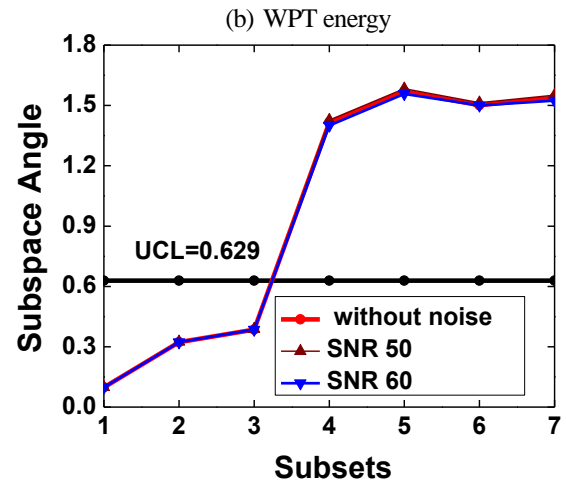
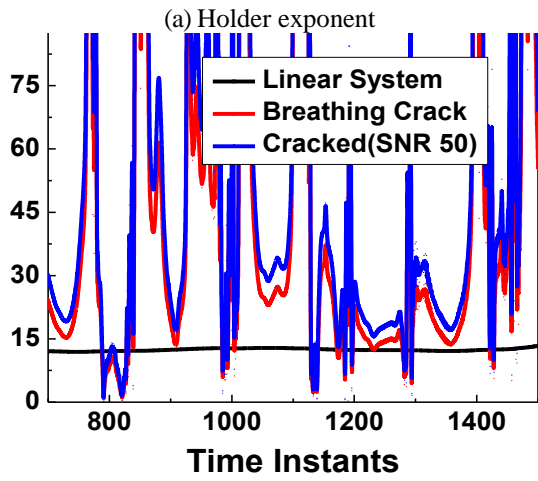
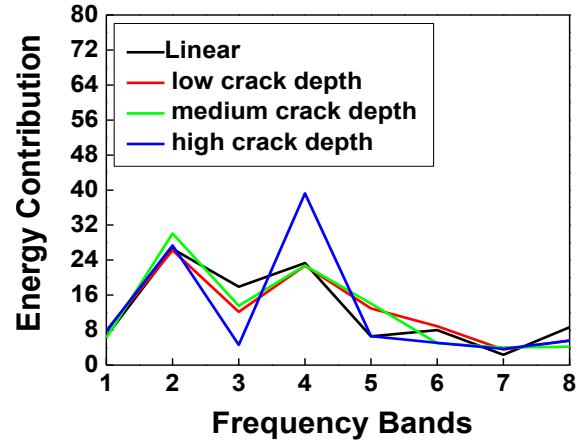
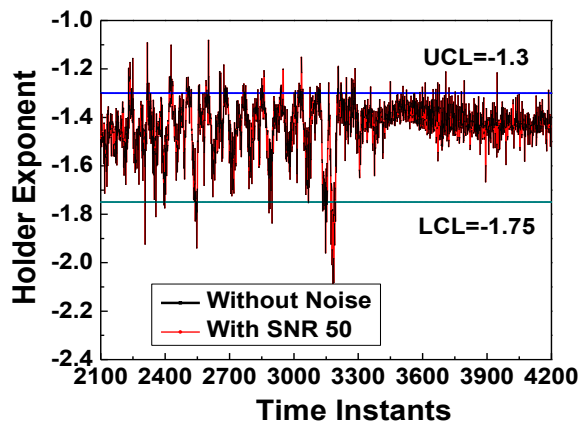


Fig. 6 Breathing Crack Problem

$$\mu = \frac{(I_u - I_d)}{I_u} \quad (21b)$$

where E, L, H indicate the Young's Modulus, length of the structure and Heaviside step function. I_u , I_d indicate the undamaged and damaged moment of inertia. Similarly K, K_d indicate the undamaged and damaged stiffness of the element

and ' μ ' ($0 < \mu < 1$) indicates the non-dimensional flexural damage. It is defined as the ratio of the loss of a moment of inertia due to damage, to the undamaged moment of inertia of the section of the beam. The value of μ corresponding to 0 and 1 indicate the healthy and completely cracked state of the section respectively. More details related to finite element modelling of breathing crack problem can be found in (Kerschen *et al.* 2014).

Table 3 WPT correlation of breathing crack problem with varied degrees of nonlinearity

| Crack Depth | Frequency bands corresponding to the 3 rd level of WPT decomposition | | | | | | | | Average |
|--------------|---|--------|--------|--------|--------|--------|--------|---------|----------|
| | 1 | 2 | 3 | 4 | 5 | 6 | 7 | 8 | |
| Low | 0.0119 | 0.1046 | 0.4142 | 0.1053 | 0.2979 | 0.1466 | 0.0975 | 0.33505 | 0.189131 |
| Medium | 0.2249 | 0.1243 | 0.0894 | 0.0324 | 0.0563 | 0.1906 | 0.0718 | 0.2026 | 0.1240 |
| High | 0.0281 | 0.0675 | 0.0569 | 0.0306 | 0.2614 | 0.0738 | 0.0685 | 0.2914 | 0.1098 |
| High(SNR 50) | 0.0221 | 0.0524 | 0.0521 | 0.0306 | 0.2614 | 0.0738 | 0.0558 | 0.2422 | 0.0988 |

Table 4 Test data details

| Label | State Condition | description |
|----------|--------------------------------|--------------------|
| State 1 | Undamaged | Baseline condition |
| State 10 | Nonlinearity Induced (damaged) | Gap (0.2 mm) |
| State 14 | Nonlinearity Induced (damaged) | Gap (0.05 mm) |

Table 5 WPT correlation of LANL 4DOF benchmark

| Datasets | Frequency bands corresponding to the 3 rd level of WPT decomposition | | | | | | | | Average |
|----------|---|--------|--------|---------|--------|--------|--------|---------|---------|
| | 1 | 2 | 3 | 4 | 5 | 6 | 7 | 8 | |
| State 1 | 0.7875 | 0.6624 | 0.6113 | 0.8912 | 0.8121 | 0.8353 | 0.8739 | 0.8898 | 0.7954 |
| State 10 | 0.4252 | 0.1868 | 0.2904 | 0.0316 | 0.1838 | 0.0396 | 0.4673 | 0.1332 | 0.2198 |
| State 14 | 0.6491 | 0.2805 | 0.0601 | 0.06715 | 0.1605 | 0.3325 | 0.0816 | 0.02162 | 0.2067 |

The breathing crack phenomenon is introduced after 2200 time steps in a linear cantilever beam with non-dimensional flexural damage, $\mu = 0.4$. (i.e., crack depth, $a=0.156567d=2.2$ mm) and after 3200 time steps a higher level of crack width $\mu = 0.8$ (i.e., crack depth, $a=0.415d = 5.8$ mm) is simulated for nonlinear phenomena. The beam is excited at node 11 with a 1.0s constant amplitude ambient excitation of 2NRMS in the frequency band [1–600 Hz]. The chosen sampling frequency is 5000 Hz. The first five natural frequencies of the underlying linear cantilever beam, i.e., without the breathing crack, are 11.73 Hz, 73.54 Hz, 205.96 Hz, 403.87 Hz, and 668.67 Hz.

The results corresponding to various nonlinear indicators obtained from the numerical investigations carried out on the breathing crack problem are shown in Fig. 6. While the time-frequency plots are shown in Figs. 6(a)-6(c), the plots related to multivariate analysis (i.e., PCA and Null subspace) are shown in Figs. 6 (d)-6(f).

The holder exponent plot shown in Fig. 6(a) indicates that the holder exponent values cross the limit of linearity at the onset of nonlinearity (i.e., at two time steps 2200th and 3200th time instant). The drop value at the initiation of nonlinearity (i.e., at 2200th time step with lower crack depth) is relatively smaller when compared to the drop at the higher crack depth (i.e., at 3200th time step). The ratio of drop levels is found to be 2.3 which incidentally relates closely to the ratio of crack depths. Even though we can arrive at the level of nonlinearity present in the system using the holder exponent for this problem, it is difficult to generalize it to all problems, unlike null subspace analysis demonstrated in section 3.1.

The instantaneous frequency corresponding to the uncracked and the breathing crack cantilever problem is shown in Fig. 6(c). It is clear that the Instantaneous frequency of the uncracked beam (linear) is constant around the fundamental resonant frequency of the linear system (i.e., 11.73 Hz). However, the instantaneous frequency of the cantilever beam with a breathing crack oscillates periodically between the values corresponding to the fully open and fully closed crack states. Similar observations can be made even with the noisy measurements presented in Fig. 6(c).

The subspace angle computed for the breathing crack problem using PCA is shown in Fig. 6(d). The initial three subsets are without a breathing crack and, therefore, the structure is in a linear state. Hence, the subspace angles corresponding to these three subsets are well below the upper control limit. Subsequently, when the breathing crack is formed (i.e., subset 4), the nonlinearity sets into the system and It is clearly reflected in the plot shown in Fig. 6(e) by way of exceeding the established control limits. Further, it can be observed that the variation in the subspace angle cannot reflect the severity of nonlinearity present in the system as the subspace angle is marginally lower at 7th subset when the crack depth is increased.

In contrast to the above, the residual projection error obtained using PCA, and shown in Fig. 6(e), shoots up with an increase in the severity of nonlinearity. We can clearly establish the exact time instant at which the degree of nonlinearity is varied from a lower level to a higher level. The studies presented here clearly indicate that two criteria presented using principal component analysis provides a very robust method for detection of nonlinearity in a structure and are shown not to be adversely affected by noise in the measurement data.

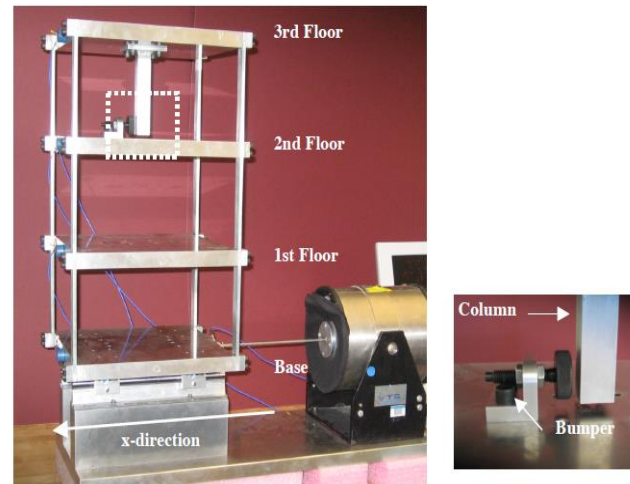


Fig. 7 Cantilever beam with a breathing crack

The studies carried out using Null subspace analysis is found to be effective in establishing the degree of nonlinearity much more precisely than the other methods. For example, from Fig. 6(f), we can clearly observe that the null subspace angle and the degree of nonlinearity indices are within the control limit for the initial three subsets due to the linear behaviour of the structure and after the fourth dataset, the indices increases with the increase in the severity of nonlinearity. The degree of nonlinearity can be estimated from the DoN plot more precisely than the subspace angle plot shown in Fig. 6(f).

All the time-frequency and multivariate analysis proposed in this paper detect the presence of damage induced nonlinearity (i.e breathing crack) even if the system exhibits a low degree of nonlinearity (i.e lower crack depth). Further, all these techniques give indirect information about the severity of the breathing crack present in the structure by its increase in its magnitude with increase in crack depth.

3.3 Experimental example: 4 DOF LANL benchmark

The LANL 4DOF frame structure shown in Fig. 7 consists of aluminium columns and plates assembled using bolted joints. The structure slides on rails that allow movement in the x-direction only. At each floor, four aluminium columns (17.7x2.5x0.6 cm) are connected to the top and bottom aluminium plates (30.5x30.5x2.5 cm) to form a complete system. Additionally, a centre column (15.0x2.5x2.5 cm) is suspended from the top floor. This column can be used to simulate damage by inducing nonlinear behaviour when it contacts a bumper mounted on the next floor.

The position of the bumper can be adjusted to vary the extent of impacting that occurs at a particular excitation level. An electrodynamic shaker provides lateral excitation to the base floor along the centerline of the structure. The structure and shaker are mounted together on an aluminium base plate (76.2x30.5x2.5 cm) and the entire system rests on rigid foam. The foam is intended to minimize extraneous sources of unmeasured excitation from being introduced through the base

of the system. A load cell with a nominal sensitivity of 2.2 mV/N was attached at the end of a stinger to measure the input force applied by the shaker. Four accelerometers with a sensitivity of 1000 mV/g each were attached to the level plate side as shown in Fig. 7. Because of the chosen location, the accelerometers are insensitive to torsional modes. Nonlinearity is simulated by a bumper mechanism that causes a repetitive, impact-type nonlinearity. This mechanism was intended to simulate, for instance, a crack that opens and closes under dynamic loads, or loose connections that rattle. As shown in Fig. 5(b), adjusting the gap between the bumper and the suspended column controls the level of nonlinearity. Therefore, the gap was varied (0.2 mm-state 10, 0.05 mm-state 14 and undamaged- state 1) in order to introduce different levels of nonlinearities. The details of the test data are shown in Table 4.

The time-frequency and multivariate analysis based nonlinear indicator plots for benchmark problem are shown in Figs. 8 (a)-8(f). The following observations can be made from the results furnished

- i. The holder exponent shown in Fig. 8(a) between state 1 and state 10 of the system indicates that state 10 data crosses the control limit and confirms the presence of nonlinearity in the structure.
- ii. The clear-cut variation in the WPT energy contribution between the two damaged states in Fig. 8(b) indicates the presence of nonlinearity. Further, the correlation coefficient corresponding to two different nonlinear datasets in (Table 5) shows poor correlation for the cases with introduced nonlinearity in comparison to the linear scenario.
- iii. The instantaneous frequency for the LANL 4 DOF problem shown in Fig. 8(c) shows a step change from 54.25 Hz to 58 Hz associated with the introduced nonlinearity.
- iv. The nonlinear indicators based on multivariate analysis i.e. PCA and NSA shown in Figs. 8(d)-8(f) respectively, also detect nonlinearity in the system by the exceedance in the corresponding nonlinearity index values against set limits.

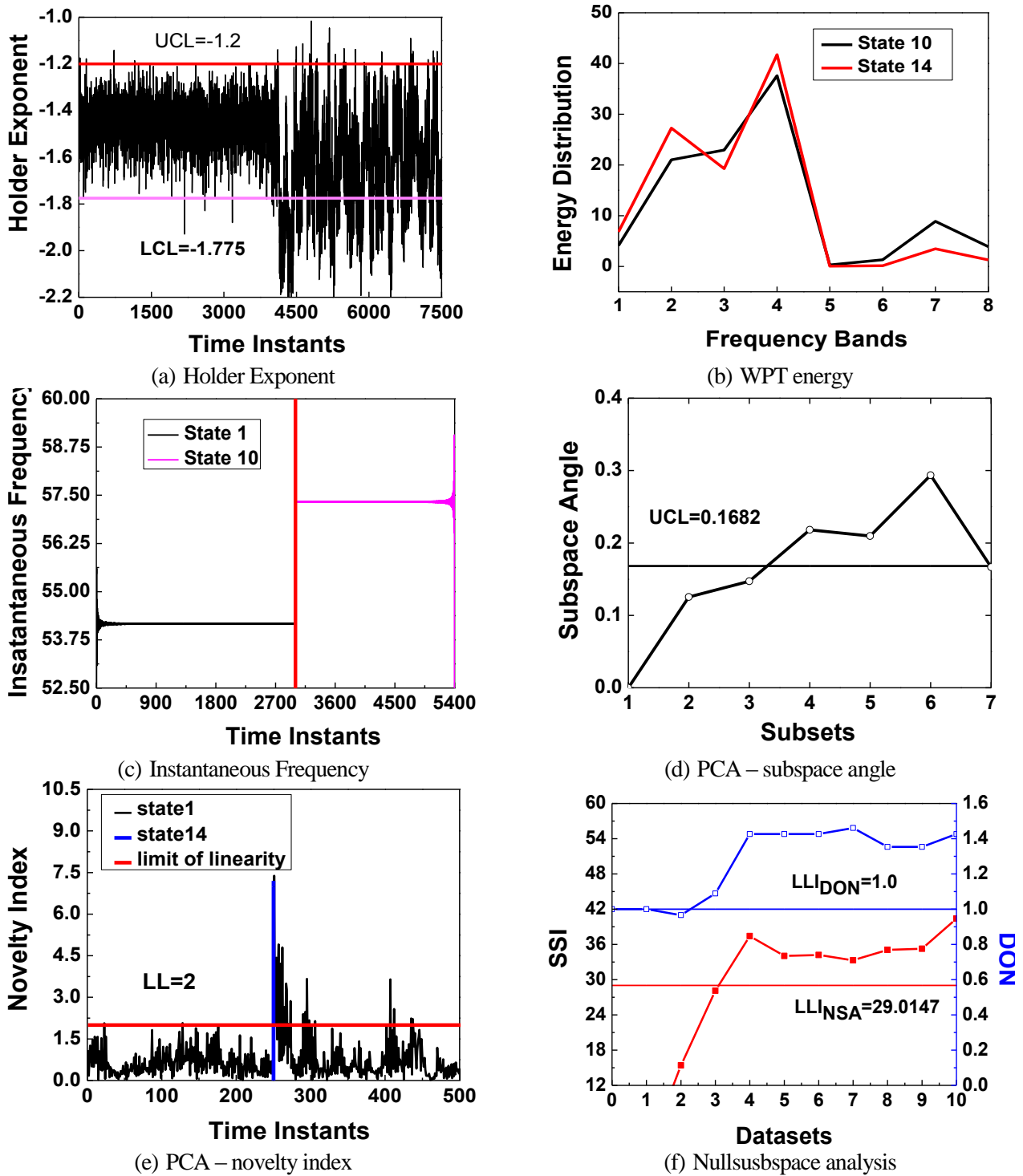


Fig. 8 LANL 4DOF Problem

4. Conclusions

In this paper, the effectiveness of time-frequency and multivariate analysis for detection of nonlinear behaviour of engineering structures using ambient vibration data is explored. Both damage induced nonlinearity and structure exhibiting nonlinear behaviour in its initial healthy state are considered in our investigations. Efforts are made to

investigate the strengths and weaknesses of each of the algorithm through numerically simulated examples followed by an experimental verification. The sensitivity of each of the algorithm with respect to measurement noise is also established. Based on the studies presented in this paper, the following conclusions can be drawn.

The Holder exponent method was shown to be effective in identifying the presence of nonlinearity introduced in the

form of discontinuities. The holder exponent has the ability to identify both class of nonlinearity (i.e., damage induced nonlinearity and inherent structural nonlinearity). It can identify the exact time instant of nonlinearity. It is also shown through investigations that the method is insensitive to measurement noise. Although the presence of nonlinearity can be established from a single sensor measurement using holder exponent, it should be ensured that the sensor is located near the source of nonlinearity present in the structure in order to capture the local nonlinear response. This may not be always practically feasible during online monitoring.

The main advantage of the wavelet packet transform is computational efficiency and immunity to noise. However, the selection of scale and level for the wavelet decomposition are critical for correct interpretation of the results. The variations in the Wavelet Packet component energy cannot alone establish the presence of nonlinearity, supplementary information from WPT cross-correlation data is required which is usually not available for real structures. The onset of nonlinearity cannot be determined by this technique. This technique requires a wide range of excitation responses for inherent local nonlinearity identification. Hence, the wavelet packet component energy is better suited for damage induced nonlinearity identification (which does not require varied excitation responses) than inherent structural nonlinearity identification.

Although shifts in the instantaneous frequency can be used as an indicator of nonlinearity, the level of nonlinearity should be significant to make these shifts recognizable. However, this method can identify the onset of nonlinearity.

The method based on PCA appears to be suitable approach considered in this paper. The PCA-based method uses response time history without further signal processing and is practically insensitive to measurement noise. The PCA technique also has the ability to identify the exact time instant of nonlinearity.

The null subspace analysis based method appears to be the most suitable method among all the techniques discussed in this paper. The null subspace angle indicator is used to determine the presence of nonlinearity in the system whereas the DoN index is used to determine the level of nonlinearity. The major advantage of the Nullspace method is that it can be easily applied to relatively large structures with a limited number of sensors. It requires analyzing the vibration signal at different instants rather than considering snapshots as in classical PCA. In this manner, the defined hyperplane contains all modal information (e.g., natural frequencies and mode shapes) while the hyperplane defined by PCA contains only mode shape information. Hence, the null subspace-based method can identify even very marginal levels of nonlinearity.

Acknowledgments

This paper is being published with the permission of the Director, CSIR-Structural Engineering Research Centre (SERC), Chennai.

References

- Bae, S.H., Jeong, W.B., Cho, J.R. and Lee, S.H. (2017), "Transient response of vibration systems with viscous-hysteretic mixed damping using Hilbert transform and effective eigenvalues", *Smart Struct. Syst.*, **20**(3), 263-272.
- Cammarata, M., Rizzo, P., Dutta, D. and Sohn, H. (2010), "Application of principal component analysis and wavelet transform to fatigue crack detection in waveguides", *Smart Struct. Syst.*, **6**(4), 349-362.
- Casciati, F. and Faravelli, L. (2016), "Dynamic transient analysis of systems with material nonlinearity: a model order reduction approach", *Smart Struct. Syst.*, **18**(1), 1-16.
- Feldman, M. (2011), "Hilbert Transform Applications in Mechanical Vibration", *Wiley-Interscience*, New York, March.
- Giannini, O., Casini, P. and Vestroni, F. (2013), "Nonlinear harmonic identification of breathing cracks in beams", *Comput. Struct.*, **129**, 166-177.
- Goggins, J., Broderick, B.M., Basu, B. and Elghazouli, A.Y. (2007), "Investigation of the seismic response of braced frames using wavelet analysis", *Struct. Control Health Monit.*, **14**, 627-648.
- Gokhale, M.Y. and Khanduja, D.K. (2010), "Time domain signal analysis using wavelet packet decomposition approach", *Int. J. Commun. Network Syst. Sci.*, **3**, 321.
- Golub, G.H. and Loan, C.F.V. (2012), "Matrix computations", **3**, (JHU Press).
- Hasselmann, T.K., Anderson, M.C. and Gan, W.E.N.S.H.U.I. (1998), "Principal components analysis for nonlinear model correlation, updating and uncertainty evaluation", *Proceedings of the 16th international modal analysis conference*, **3243**, 644.
- Hickey, D., Worden, K., Platten, M.F., Wright, J.R. and Cooper, J. E. (2009), "Higher-order spectra for identification of nonlinear modal coupling", *Mech. Syst. Signal Pr.*, **23**, 1037-1061.
- Hot, A., Kerschen, G., Foltête, E. and Cogan, S. (2012), "Detection and quantification of non-linear structural behaviour using principal component analysis", *Mech. Syst. Signal Pr.*, **26**, 104-116.
- <http://institute.lanl.gov/ei/software-and-data/data>
- Huang, N.E., Shen, Z., Long, S.R., Wu, M.C., Shih, H.H., Zheng, Q., Yen, N.C., Tung, C.C. and Liu, H.H. (1998), "The empirical mode decomposition and the Hilbert spectrum for nonlinear and non-stationary time series analysis", *Proceedings of the Royal Society of London A: mathematical, physical and engineering sciences*, **454**, 903-995.
- Lim, H.J., Kim, Y., Sohn, H., Jeon, I. and PLiu, P. (2017), "Reliability improvement of nonlinear ultrasonic modulation based fatigue crack detection using feature-level data fusion", *Smart Struct. Syst.*, **20**(6), 683-696
- Kerschen, G., Boe, P.D., Golinval, J.C. and Worden, K. (2004), "Sensor validation using principal component analysis", *Smart Mater. Struct.*, **14**, 36-42.
- Kerschen, G., Worden, K., Vakakis, A.F. and Golinval, J.C. (2006), "Past, present and future of nonlinear system identification in structural dynamics", *Mech. Syst. Signal Pr.*, **20**, 505-592.
- Khoshnoudian, F. and Talaei, S. (2017), "A new damage index using FRF data, 2D-PCA method and pattern recognition techniques", *Int. J. Struct. Stab. Dynam.*, **17**(8), 1750090.
- Khoshnoudian, F. and Bokaeian, V. (2017), "Damage detection in plate structures using frequency response function and 2D-PCA", *Smart Struct. Syst.*, **20**(4), 427-440.
- Li, L., Qin, H. and Niu, Y. (2017), "Wavelet-based system identification for a nonlinear experimental model", *Smart Struct. Syst.*, **20**(4), 415-426.
- Nagarajaiah, S. and Yang, Y. (2015), "Blind modal identification of output-only non-proportionally-damped structures by time-

- frequency complex independent component analysis”, *Smart Struct. Syst.*, **15**(1), 81-97.
- Pai, P.F., Nguyen, B.A. and Sundaresan, M.J. (2013), “Nonlinearity identification by time-domain-only signal processing”, *Int. J. Nonlinear Mech.*, **54**, 85-98.
- Prawin, J. and Rao, A.R.M. (2017), “Nonlinear identification of MDOF systems using Volterra series approximation”, *Mech. Syst. Signal Pr.*, **84**, 58-77.
- Prawin, J. and Rao, A.R.M. (2018a), “Nonlinear structural damage detection based on adaptive volterra filter model”, *Int. J. Struct. Stab. Dynam.*, **18**(2), 1871003.
- Prawin, J. and Rao, A.R.M. (2018b), “A method for detecting damage-induced nonlinearity in structures using weighting function augmented curvature approach”, *Struct. Health Monit.*, 147592171878 8801.
- Prawin, J., Rao, A.R.M. and Lakshmi, K. (2015), “Nonlinear identification of structures using ambient vibration data”, *Comput. Struct.*, **154**, 116-134.
- Prawin, J., Rao, A.R.M. and Lakshmi, K. (2016), “Nonlinear parametric identification strategy combining reverse path and hybrid dynamic quantum particle swarm optimization”, *Nonlinear Dynam.*, **84**(2), 797-781
- Rao, A.R.M., Kasireddy, V., Gopalakrishnan, N. and Lakshmi, K. (2015), “Sensor fault detection in structural health monitoring using null subspace-based approach”, *J. Intel. Mat. Syst. Str.*, **26**(2), 172-185.
- Robertson, A.N., Farrar, C.R. and Sohn, H. (2013), “An improved statistical classifier for identifying signal discontinuities using holder exponents”, *Proceedings of the 4th International Workshop on Structural Health Monitoring*, (Stanford, CA) 13-17.
- Robertson, A., Farrar, C. and Sohn, H. (2003), “Singularity detection for structural health monitoring using holder exponents”, *Mech. Syst. Signal Pr.*, **17**, 1163-1184.
- Salehi, H., Burgueño, R., Das, S., Biswas, S. and Chakrabarty, S. (2016), “Structural health monitoring from discrete binary data through pattern recognition. Insights and Innovations in structural engineering”, *Mech. Comput.*, 1840-1845.
- Sapsis T.P., Quinn, D.D., Vakakis, A.F. and Bergman, L.A. (2012), “Effective stiffening and damping enhancement of structures with strongly nonlinear local attachments”, *J. Vib. Acoust.*, **134**, 011016.
- Shahverdi, S., Lotfollahi-Yaghin, M.A. and Asgarian, B. (2013), “Reduced wavelet component energy-based approach for damage detection of jacket type offshore platform”, *Smart Struct. Syst.*, **11**(6), 589-604.
- Sohn, H., Farrar, C.R., Hemez, F.M. and Czarnecki, J.J. (2002), “A review of structural health review of structural health monitoring literature”, *Proceedings of 3rd World Conference on Structural Control*, Como, Italy, January.
- Wang, Z.C., Geng, D., Ren, W.X., Chen, G.D. and Zhang, G.F. (2015), “Damage detection of nonlinear structures with analytical mode decomposition and Hilbert transform”, *Smart Struct. Syst.*, **15**(1), 1-13.
- Worden, K. and Tomlinson, G.R. (2000), *Nonlinearity in structural dynamics: detection, identification and modeling*, (CRC Press).
- Worden, K., Farrar, C.R., Haywood, J. and Todd, M. (2008), “A review of nonlinear dynamics applications to structural health monitoring”, *Struct. Control Health Monit.*, **15**, 540-567.
- Yan, A.M. and Golinval, J.C. (2006), “Null subspace-based damage detection of structures using vibration measurements”, *Mech. Syst. Signal Pr.*, **20**, 611-626.
- Zang, C. and Imregun, M. (2001), “Combined neural network and reduced FRF techniques for slight damage detection using measured response data”, *Arch. Appl. Mech.*, **71**(8), 525-536.

BS